Host-targeting protein 1 (SpHtp1) from the oomycete *Saprolegnia parasitica* translocates specifically into fish cells in a tyrosine-O-sulphate–dependent manner

Stephan Wawra[a], Judith Bain[b], Elaine Durward[a], Irene de Bruijn[a], Kirsty L. Minor[a], Anja Matena[c], Lars Löbach[a], Stephen C. Whisson[d], Peter Bayer[c], Andrew J. Porter[e], Paul R. J. Birch[d,f], Chris J. Secombes[g], and Pieter van West[a,1]

[a]Aberdeen Oomycete Laboratory, [b]Division of Applied Medicine, and [e]School of Medical Sciences, College of Life Sciences and Medicine, Institute of Medical Sciences, University of Aberdeen, Foresterhill, Aberdeen AB25 2ZD, United Kingdom; [c]Structural and Medicinal Biochemistry, Zentrum für Medizinische Biotechnologie, Faculty of Biology, Universität Duisburg-Essen, 45117 Essen, Germany; [d]Cell and Molecular Science, and [f]Division of Plant Sciences, College of Life Sciences, The James Hutton Institute, University of Dundee, Invergowrie, Dundee DD2 5DA, United Kingdom; and [g]Scottish Fish Immunology Research Centre, Institute of Biological and Environmental Sciences, University of Aberdeen, Aberdeen AB24 2TZ, United Kingdom

Edited by Brian J. Staskawicz, University of California, Berkeley, CA, and approved December 20, 2011 (received for review August 23, 2011)

The eukaryotic oomycetes, or water molds, contain several species that are devastating pathogens of plants and animals. During infection, oomycetes translocate effector proteins into host cells, where they interfere with host-defense responses. For several oomycete effectors (i.e., the RxLR-effectors) it has been shown that their N-terminal polypeptides are important for the delivery into the host. Here we demonstrate that the putative RxLR-like effector, host-targeting protein 1 (SpHtp1), from the fish pathogen *Saprolegnia parasitica* translocates specifically inside host cells. We further demonstrate that cell-surface binding and uptake of this effector protein is mediated by an interaction with tyrosine-O-sulfate–modified cell-surface molecules and not via phospholipids, as has been reported for RxLR-effectors from plant pathogenic oomycetes. These results reveal an effector translocation route based on tyrosine-O-sulfate binding, which could be highly relevant for a wide range of host–microbe interactions.

protein translocation | Phytophthora | *Plasmodium*

Several prokaryotic and eukaryotic microbial pathogens have evolved delivery mechanisms for pathogenicity effector proteins into host cells. Effectors modulate molecular processes in their hosts to suppress immune responses and thereby help to establish an infection (1–4). For example, pathogenic bacteria have developed a number of secretion systems that allow direct translocation of effector proteins into the cells under attack (5–7). Although bacterial translocation mechanisms are largely well characterized, little is known about how effectors from eukaryotic pathogens are delivered into host cells.

Recently, we found that SpHtp1, a putative effector from the fish pathogenic oomycete, *Saprolegnia parasitica*, is delivered by the pathogen into cells of a rainbow trout cell line (RTG-2) (8). SpHtp1 contains an Arg-His-Leu-Arg (RHLR) sequence at a position characteristic for the "RxLR motif" found in many putative effectors of plant-pathogenic oomycetes (8). Furthermore, we observed that this protein translocates into fish (RTG-2) cells in the absence of the pathogen, whereas a mutant protein lacking the amino acids 24–68, including the RHLR sequence, was unable to do so (8). However, SpHtp1 lacks the Y-W sequence element (9) that is a common of many structurally characterized oomycete RxLR-effectors (10, 11). Furthermore, with the availability of a large number of *S. parasitica* sequences (http://www.broadinstitute.org/), it has become apparent that there is no enrichment for a conserved RxLR-sequence within the secretome, as has been observed for *Phytophthora spp.* and the downy mildews (12, 13). Indeed, *S. parasitica* is phylogenetically distinct from the Peronosporales (14), in which RxLR-effectors occur abundantly (12, 15). Therefore, it is possible that SpHtp1 is not a conventional, or typical, RxLR-effector.

The most extensively studied group of oomycete effectors are the RxLR-effectors (16–20). Initially it was thought that the host translocation mechanism of these effectors shares similarities with the *Plasmodium* PEXEL translocation system (21–24). However, it has also been suggested by Kale et al. (19) that RxLR-effectors from plant pathogenic oomycetes are translocated in a pathogen-independent manner through binding to phosphorylated lipids, relying on an intact RxLR-motif that is part of a larger entity within the N-terminal leaders of the corresponding proteins. Yaeno et al. (10) tried to reproduce some of the RxLR-leader to lipid-binding observations made by Kale et al. (19), but were unsuccessful. In order for the PEXEL effectors of *Plasmodium* to translocate, it was found that the PEXEL-motif is specifically cleaved within the parasite and subsequently *N*-acetylated (25). Such PEXEL processing was shown to be important for delivery of these effectors into red blood cells via a specific translocon complex containing proteins from both the host and the parasite (25–28). At present it is unclear how oomycete RxLR effectors are translocated and opinions are divided (29).

Results and Discussion

To further investigate the mechanism underlying the translocation activity of SpHtp1 and to evaluate if this mechanism shares similarities to that described for RxLR-effectors found in plant pathogenic oomycetes, we fused the amino acids 24–68, representing a putative leader peptide, to mRFP, resulting in the reporter construct SpHtp1$^{24\text{-}68}$mRFP(His)$_6$. Like the full-length protein (8), SpHtp1$^{24\text{-}68}$mRFP(His)$_6$ was able to enter trout cells (Fig. 1*A*). In contrast, mRFP(His)$_6$ alone was not detected in trout cells using identical conditions (Fig. 2 *A* and *K*, column 1). Recently, it has been reported that several plant pathogenic oomycete RxLR-effectors enter eukaryotic cells of different origins (i.e., human and plant) in the absence of the pathogen (19). Therefore, we tested if SpHtp1$^{24\text{-}68}$mRFP(His)$_6$ is able to enter human cells (HEK293 cell line) and onion epidermal cells. However, no translocation of this protein was observed into HEK293 or onion epidermal cells (Fig. 1 *B* and *C*; see *SI Appendix*, Note 1 for further details), indicating that the translocation of this protein is host cell-specific. Both cell types were not impaired in their trafficking and endocytosis abilities (*SI Appendix*, Fig. S2).

Author contributions: S.W., P.B., A.J.P., P.R.J.B., C.J.S., and P.v.W. designed research; S.W., J.B., E.D., I.d.B., K.L.M., A.M., L.L., and P.v.W. performed research; S.C.W., P.B., A.J.P., P.R.J.B., C.J.S., and P.v.W. contributed new reagents/analytic tools; S.W., P.B., and P.v.W. analyzed data; and S.W., I.d.B., S.C.W., P.R.J.B., C.J.S., and P.v.W. wrote the paper.

The authors declare no conflict of interest.

This article is a PNAS Direct Submission.

[1]To whom correspondence should be addressed. E-mail: p.vanwest@abdn.ac.uk.

This article contains supporting information online at www.pnas.org/lookup/suppl/doi:10.1073/pnas.1113775109/-/DCSupplemental.

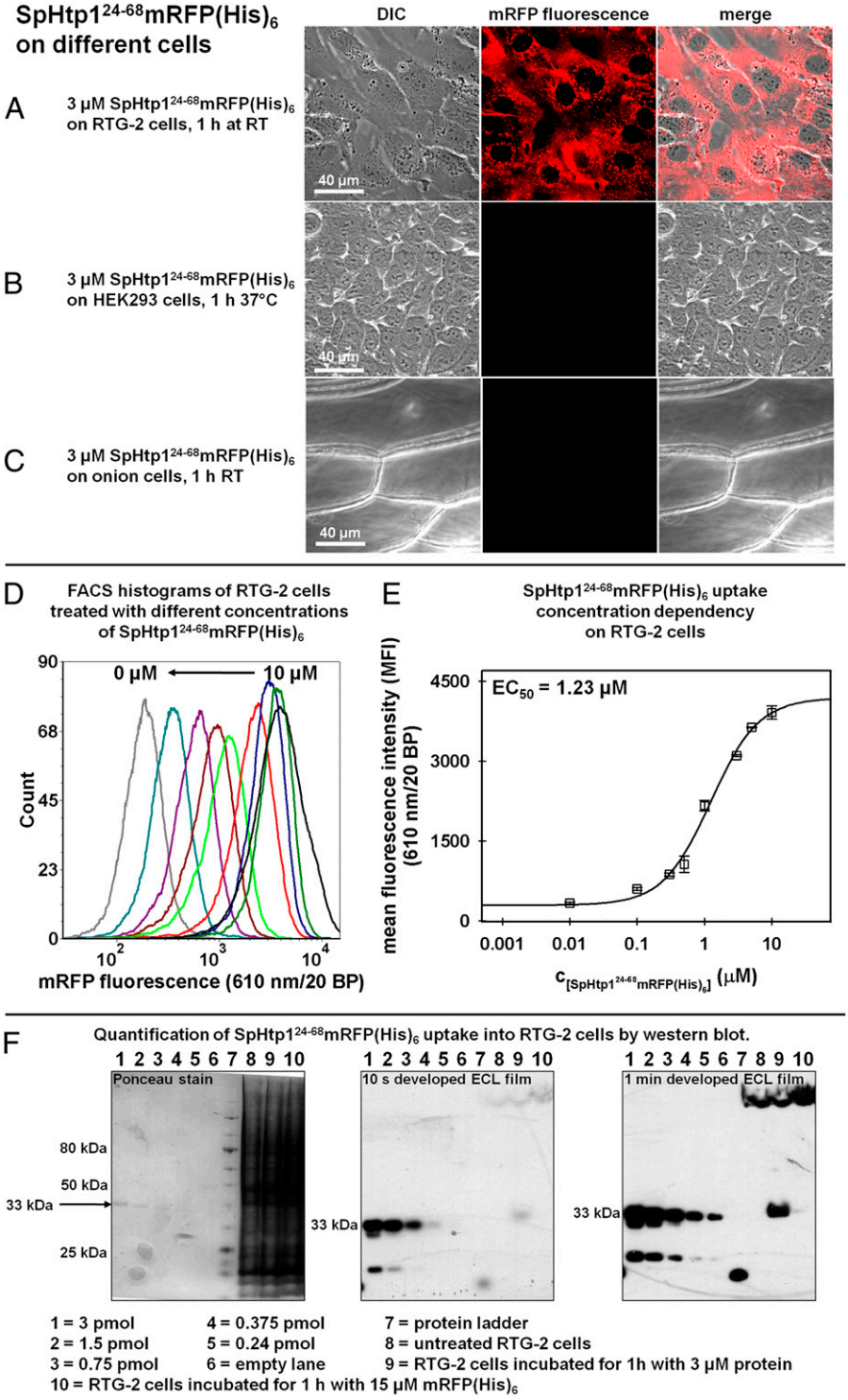

Fig. 1. The N-terminal leader peptide of SpHtp1 (amino acids 24–68) shows host cell-specific translocation. (*A*–*C*) The SpHtp1 leader fusion protein shows an autonomous translocation activity on the rainbow trout gonad cell line RTG-2 (*A*) but not with the human derived HEK293 cell line (*B*) or onion epidermis cells (*C*). Cells were incubated for 1 h with 3 μM SpHtp1$^{24-68}$mRFP(His)$_6$ in L15-medium containing 10% FCS for the RTG-2 cells, in DMEM-medium (+10% FCS) for the HEK293 cells and in PBS containing 10% BSA for the onion epidermis cells at the indicated temperatures. Red channel: mRFP fluorescence; white channel: differential interference contrast (viability controls can be found in *SI Appendix*, Figs. S2 and S4). (*D*) Flow cytometry histograms for one repeat of the concentration dependency measurement. The RTG-2 cells were treated for 1 h at room temperature with either 10 μM (black), 5 μM (dark green), 3 μM (dark blue), 1 μM (red), 0.5 μM (green), 0.3 μM (brown), 0.1 μM (dark red), 0.01 μM (magenta), and 0 μM (gray) SpHtp1$^{24-68}$mRFP(His)$_6$. From 10,000 counted events, a homogenous population of cells that were TO-PRO-3 iodide-negative was selected (on average ~80% of all events) and further analyzed. (*E*) EC$_{50}$ determination of SpHtp1$^{24-68}$mRFP(His)$_6$ uptake into RTG-2 cells using the MFI from the FACS histograms (exemplarily shown in *D*). The errors are the SDs of the MFI values from three independent experiments. The obtained EC$_{50}$ was 1.23 μM SpHtp1$^{24-68}$mRFP(His)$_6$. (*F*) Quantification of SpHtp1$^{24-68}$mRFP(His)$_6$ translocation into RTG-2 cells by Western blotting. Samples were prepared as described for FACS analyses then, following trypsination, the cells were harvested by centrifugation and resuspended 2× in PBS to remove excess trypsin. The wet cell pellets containing ~2 × 10^6 cells (~20 μL) were lysed at 95 °C in 100 μL of Laemmli sample buffer containing 8 M urea, 2% β-mercaptoethanol, and 1 mM PMSF. Sample volume loaded was 15 μL. (Lanes 1–5) A total amount of 3 pmol (lane 1), 1.5 pmol (lane 2), 0.75 pmol (lane 3), 0.375 pmol (lane 4), and 0.24 pmol (lane 5) of purified SpHtp1$^{24-68}$mRFP(His)$_6$ was loaded. Lane 6 was kept empty. Lane 8 contained a sample of RTG-2 cells incubated without protein, and lane 9 contained a RTG-2 cells incubated for 1 h with 3 μM SpHtp1$^{24-68}$mRFP(His)$_6$. Lane 10 shows a sample incubated for 1 h with 15 μM mRFP(His)$_6$. (*Left*) Ponceau stain of the proteins after transfer onto a nitrocellulose membrane. (*Center* and *Right*) ECL films after 10-s and 1-min development, respectively. The amount of SpHtp1$^{24-68}$mRFP(His)$_6$ was determined by densitometric analysis of the band at 33 kDa and resulted in a value of ~0.4 pmol.

To investigate whether the observed translocation activity of SpHtp1$^{24-68}$mRFP(His)$_6$ is dependent on a molecule present on the cell surface or based on an intrinsic physical property of this polypeptide, the concentration-dependent uptake into RTG-2 cells after 1 h was analyzed using flow cytometry (Fig. 1 *D* and *E*). Plotting mean fluorescence intensity (MFI) values against the respective protein concentration yielded a sigmoid shaped distribution indicative of a saturable entry system, possibly a receptor. The presence of the lag phase rules out a solely diffusion-driven process. The EC$_{50}$ value for the SpHtp1$^{24-68}$mRFP(His)$_6$ uptake was calculated to be 1.23 μM. Furthermore, Western blot analysis was used to estimate the absolute amount of SpHtp1$^{24-68}$mRFP(His)$_6$ that can be translocated inside the RTG-2 cells after 1-h incubation (Fig. 1*F*). The results show that SpHtp1$^{24-68}$mRFP(His)$_6$ is not degraded inside the cells and the densitometric analysis of the band detected at 33 kDa led to a value of ~0.4 pmol that was loaded onto the gel. Using the average volume of a trypsinated RTG-2 cell of 1,770 μm^3 (determined by measuring cell diameters and assuming a perfect spherical shape), an average of ~2.7 × 10^{13} molecules of SpHtp1$^{24-68}$mRFP(His)$_6$ per cell were found under the given

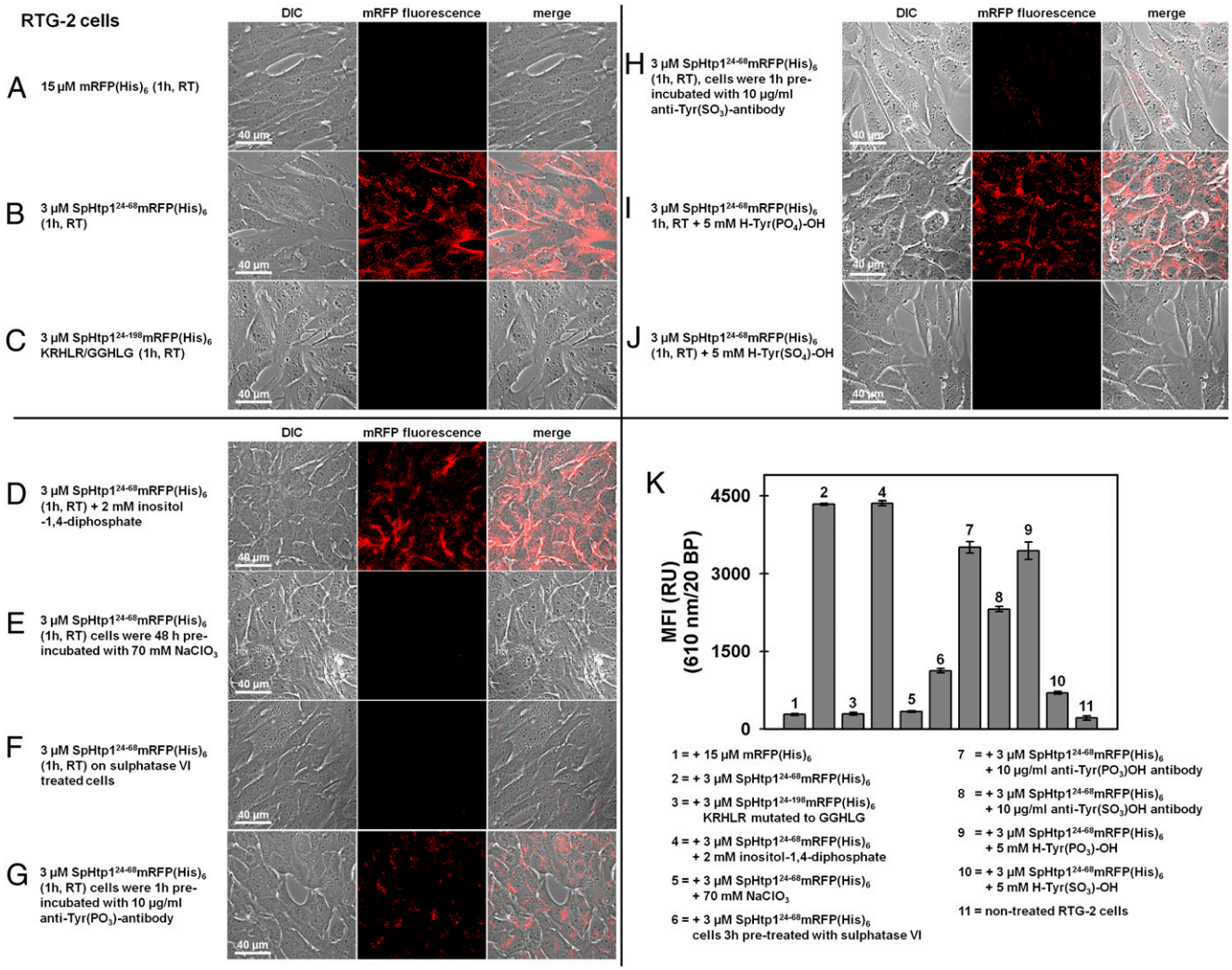

Fig. 2. The translocation activity of the SpHtp1 is dependent on sulfate-modified cell-surface molecules. (*A–J*) Confocal microscopy images of RTG-2 cells: Cells incubated for 1 h with 15 µM mRFP(His)$_6$ (*A*) did not show any mRFP fluorescence inside the cells in contrast to cells incubated with 3 µM SpHtp1$^{24\text{-}68}$mRFP(His)$_6$ (*B*). The mutated full-length SpHtp1-mRFP fusion protein, in which the KRHLR amino acids had been substituted with GGHLG, did not show any translocation into the cells under identical conditions (*C*). The reported RxLR-protein translocation inhibitor inositol-1,4-diphosphate (19) did not affect the translocation of SpHtp1$^{24\text{-}68}$mRFP(His)$_6$ (*D*). However, pretreatment of the cells for 48 h with 70 mM of the sulfotransferase inhibitor $NaClO_3$ (30) strongly inhibited the translocation of this protein (*E*). A similar effect was observed when the cells were 3-h preincubated with 1.1 U of a type VI aryl-sulphatase from *Aerobacter aerogenes* (34) (*F*). Incubation of the cells for 1 h with 10 µg/mL of an antityrosine-phosphate specific antibody before the application of SpHtp1$^{24\text{-}68}$mRFP(His)$_6$ only slightly reduced the uptake of this protein (*G*). A much stronger effect was observed when an anti-tyrosine-sulfate specific antibody was used under identical conditions (*H*). Using the modified tyrosine amino acid H-Tyr(PO_3)-OH at a concentration of 5 mM to compete for the SpHtp1$^{24\text{-}68}$mRFP(His)$_6$ binding, the fluorescence levels found inside the cells were not significantly affected compared with the control (*I*). In contrast, with the same amount of tyrosine-sulfate [H-Tyr(SO_3)-OH] a much stronger inhibitory effect was observed (*J*). Red channel: mRFP fluorescence; white channel: differential interference contrast (viability controls can be found in *SI Appendix*, Fig. S4). (*K*) Flow cytometric quantification of the mRFP-fluorescence uptake into RTG-2 cells corresponding to the images shown in *A–J*. Cells were grown in 25-cm^2 flasks and washed 5× with L15 medium before incubation with the respective protein concentration dilute in L15-medium containing 10% FCS. After 1-h incubation, the cells were washed 3× 5 min with PB), 1× 10 min with PBS containing TO-PRO-3 iodide in a 1:1,000 dilution, 2× 5 min with PBS adjusted to pH 5.5, and 2× 5 min with PBS adjusted to pH 8.5. Subsequently, the cells were detached with 1 mL of 0.5 mg/mL trypsin (+1 mM EDTA), resulting in samples with ~2×10^6 cells/mL. From 10,000 events counted, a homogenous population of cell that were TO-PRO-3 iodide-negative was selected (on average ~80% of all events) and further analyzed. Plotted are the MFI values averaged from three individual experiments. Error bars are the SD of the MFI values. Cells were incubated with 15 µM mRFP(His)$_6$ (column 1), 3 µM SpHtp1$^{24\text{-}68}$mRFP(His)$_6$ (column 2), 3 µM of the SpHtp1$^{24\text{-}198}$mRFP(His)$_6$GGHLG mutant (column 3), or 3 µM SpHtp1$^{24\text{-}68}$mRFP(His)$_6$ in combination with the indicated treatments (columns 5–10) or nontreated RTG-2 cells (column 11). Example raw data for one repeat can be found in the *SI Appendix*.

conditions. Therefore, when assuming an average surface accessibility of the cells to the protein solution of 100%, and only a limitation by diffusion, the minimal concentration for the SpHtp1$^{24\text{-}68}$mRFP(His)$_6$ corresponding receptor present at any time on the cell surface can be estimated at ~12 fmol per cell/s.

Recently it was reported that the translocation of some plant pathogenic oomycete and fungal effectors is dependent on RxLR and RxLR-like motifs and their ability to interact with inositol-phosphate derivatives. It has been reported that the phospholipid head-groups inositol-1,3-bisphosphate (I1,3P2) and inositol-1,4-bisphosphate (I1,4P2) are efficient inhibitors of the RxLR-mediated translocation process, exhibiting nano-molar binding constants to the reported polypeptides (19). The translocation activity of the SpHtp1-leader was also dependent on the KRHLR amino acids, because a full-length mRFP fusion protein, SpHtp1$^{24\text{-}198}$ mRFP(His)$_6$ GGHLG, in which the KRHLR amino acids were

mutated to GGHLG did not enter RTG-2 cells (compare Fig. 2 *B* and *C*, and *K*, columns 2 and 3). However, even though the translocation activity is embedded within the protein N terminus and mutation of the KR(HL)R amino acids disabled translocation, the SpHtp1 N-terminal polypeptide did not show any affinity to phospholipids when tested on lipid spot membranes (*SI Appendix*, Fig. S3*A*). Similar observations were recently published for the RxLR-effectors AVR3a from *Phytophthora infestans*, AVR1b from *Phytophthora sojae*, and AVR1b and AVR3a4 from *Phytophthora capsici* (10). The authors showed that the RxLR-leaders of these proteins do not bind phospholipids (10), and this directly challenges the mechanism of RxLR-mediated translocation proposed by Kale et al. (19). Furthermore, the SpHtp1 protein construct lacking the N-terminal polypeptide, SpHtp1$^{69\text{-}198}$(His)$_6$, did not show any detectable phospholipid binding activity. The full-length protein construct SpHtp1$^{24\text{-}198}$(His)$_6$, lacking only the signal peptide did show an interaction on lipid-spot membranes. However, no physical interaction with the I1,3P2 and I1,4P2 head-groups could be detected by isothermal titration calorimetry (ITC) (*SI Appendix*, Fig. S3*B*). To investigate if, for example, I1,4P2 might indirectly affect the translocation of SpHtp1$^{24\text{-}68}$mRFP(His)$_6$, confocal microscopy and FACS studies were performed. With both approaches no inhibitory effect of I1,4P2 could be detected, even at concentrations exceeding fourfold the amount reported to be sufficient for RxLR-effectors of plant pathogenic oomycetes (Fig. 2 *D* and *K*, column 4) (19).

To investigate the mechanism of uptake of SpHtp1, we considered other potential cell-surface chemical modifications. Among them is tyrosine-O-sulfate, a common aryl sulfate modification presented on cell surfaces (30). This modification originates from the attachment of a sulfate group to the tyrosine side chains of proteins during their transit through the Golgi, and can be found in numerous cell-surface proteins. Furthermore, tyrosine sulphation has been shown to be essential for protein–protein associations in diverse pathogen–host interactions (31, 32). For example, the sulphation of four tyrosines in the T-cell HIV-coreceptor CCR5 is necessary for efficient binding of HIV (30). Moreover, the sulphation of two tyrosines in the RBC Duffy protein, the receptor for *Plasmodium vivax*, is crucial for merozoite invasion (33). Remarkably, translocation of SpHtp1$^{24\text{-}68}$ mRFP(His)$_6$ was found to be dependent on sulfated modifications present at the RTG-2 cell surfaces, because inhibition of sulfotransferases in the fish cells by $NaClO_3$ (30) reduced the uptake by ~30-fold (Fig. 2 *E* and *K*, column 5). In addition, the enzymatic removal of extracellular sulfate groups from aromatic residues with a type VI sulfatase (34) reduced the translocation of

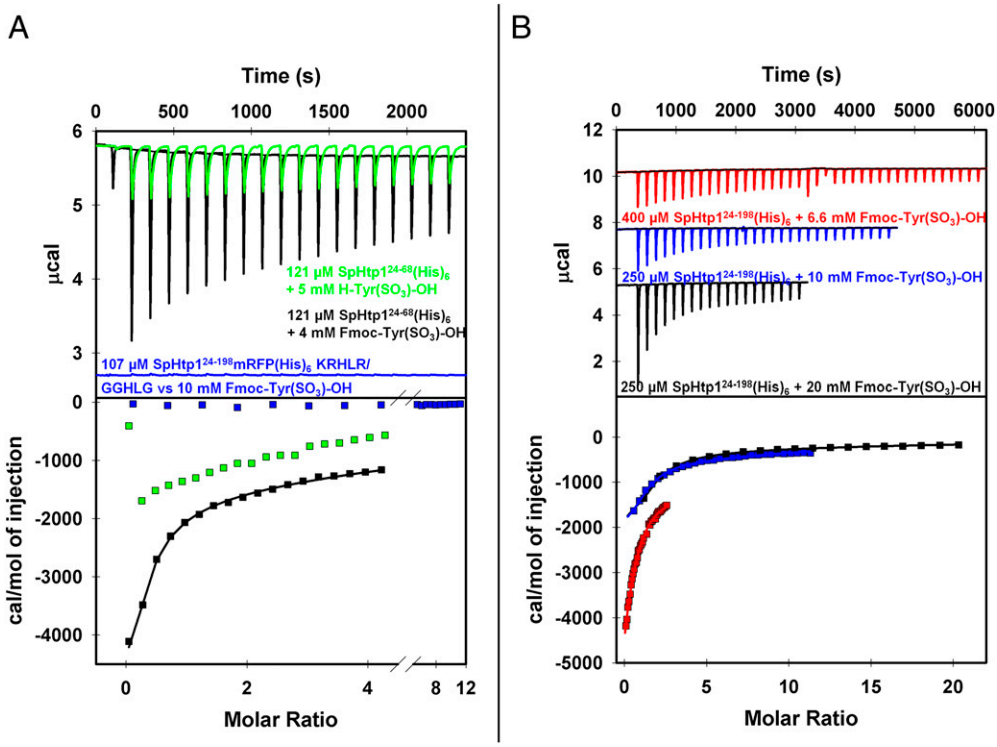

Fig. 3. The N-terminal leader of SpHtp1 directly interacts with H-Tyr(SO$_3$)-OH and Fmoc-Tyr(SO$_3$)-OH. (*A*) Green trace: Isothermal calorimetric titration measurements showed that H-Tyr(SO$_3$)-OH binds to SpHtp1$^{24\text{-}68}$mRFP(His)$_6$ in an exothermal reaction. The obtained thermogram could not be accurately fitted to a one site binding model, because of the high binding constant. However, compared with the titration carried out with Fmoc-Tyr(SO$_3$)-OH (black trace), one can assume a binding constant that is approximately three to four times weaker. Black trace: titration of Fmoc-Tyr(SO$_3$)-OH to SpHtp1$^{24\text{-}68}$mRFP (His)$_6$. The data obtained were fitted according to a single site binding model yielding values of: K_D = (116 ± 16.9) µM, (0.72 ± 0.41) binding sites, ΔH_{ITC} = (−19.2 ± 4.23) kJ·mol^{-1} and ΔS_{ITC} = 19.1 J·mol^{-1}·K^{-1}. Blue trace: titration of Fmoc-Tyr(SO$_3$)-OH to SpHtp1$^{24\text{-}198}$mRFP(His)$_6$GGHLG. No interaction between the small molecular compound and the mutated SpHtp1-mRFP construct was detected. (*B*) Titrations of different Fmoc-Tyr(SO$_3$)-OH stock concentrations to the indicated SpHtp1$^{24\text{-}198}$(His)$_6$ solutions. The data of the individual experiments were fitted and the resulting reaction parameters were averaged leading to: K_D = (144 ± 21.9) µM, (0.84 ± 0.36) binding sites, ΔH_{ITC} = (−17.6 ± 1.51) kJ·mol^{-1} and a ΔS_{ITC} = (14.4 ± 4.4) J·mol^{-1}·K^{-1}. All titrations were carried out at 25 °C with 200 µL of the indicated protein solution as bait. The indicated titrant concentrations represent the stock concentration of the ligands in the syringe. For all experiments the first titration step added 0.4 µL of the ligand solution. For all titrations shown in *A*, the first step was followed by 18× 2-µL injections, each separated by a 120-s time delay. In *B*, the black thermogram was obtained by titrating 19× 2 µL of the ligand, the blue thermogram was the result of 29× 1.35-µL injections and for the experiment represented by the red trace 39× 1-µL titration steps were carried out. All proteins were extensively dialyzed against 50 mM sodium phosphate buffer pH 7.5. The titrant solutions were always freshly prepared with the corresponding dialysis buffer. Before fitting, all thermograms were baseline corrected and subtracted with the thermograms of the corresponding blank titrations (titrant into buffer).

SpHtp1$^{24-68}$mRFP(His)$_6$ by 80% (Fig. 2 *F* and *K*, column 6). To show that the RTG-2 cells were not impaired by the $NaClO_3$ or sulfatase treatment, control experiments using the Alexa Fluor 488-labeled lectin wheat germ agglutinin (WGA) were performed (35). Coincubation of SpHtp1$^{24-68}$mRFP(His)$_6$ with WGA on RTG-2 cells lead to overlapping fluorescence signals of both labels (mRFP and Alexa Fluor 488) in vesicular structures close to the nuclei of the cells (*SI Appendix*, Fig. S4*A*). Although pretreatment of the RTG-2 cells with either $NaClO_3$ or aryl-sulfatase strongly reduced the uptake of SpHtp1$^{24-68}$mRFP(His)$_6$, in the coincubation experiments the uptake of WGA remained unaffected (*SI Appendix*, Fig. S4 *B–F*). In addition, the ability of an antibody that specifically binds tyrosine-O-sulfate to block the SpHtp1$^{24-68}$mRFP(His)$_6$ uptake was tested, and compared with an antibody specific for the very similar tyrosine-phosphate moiety. The RTG-2 cells were preincubated with 10 μg/mL of the respective antibodies at room temperature for 1 h before exposure to 3 μM SpHtp1$^{24-68}$mRFP(His)$_6$. Under these conditions, the antityrosine-phosphate antibody reduced the translocation by ∼20% (Fig. 2 *G* and *K*, column 7), and the antityrosine-sulfate specific antibody blocked the uptake by ∼50% (Fig. 2 *H* and *K*, column 8). Complementary experiments using the corresponding modified amino acids, H-Tyr(PO_3)-OH and H-Tyr(SO_3)-OH at a concentration of 5 mM to compete for SpHtp1$^{24-68}$mRFP(His)$_6$ binding to the cells showed that the presence of H-Tyr(PO_3)-OH reduced the uptake by ∼20% (Fig. 2 *I* and *K*, column), whereas H-Tyr(SO_3)-OH under the same conditions blocked the translocation by ∼90% (Fig. 2 *J* and *K*, column 10). The discrepancy of the inhibitory effect of the "bulky" tyrosine-sulfate specific antibody and H-Tyr(SO_3)-OH probably arises from the fact that, as a large number of different proteins on the cell surface are tyrosine-O-sulfate–modified (36), the antibody will not only bind to the SpHtp1 receptor but also to all other accessible epitopes.

ITC experiments were used to investigate the potential and affinity of the SpHtp1 to interact with the tyrosine-O-sulfate moiety. SpHtp1$^{24-68}$mRFP(His)$_6$ showed an exothermal interaction with an estimated binding constant of 400–500 μM toward H-Tyr(SO_3)-OH (Fig. 3*A*, green trace). In control experiments using tyrosine phosphate, no binding of this compound to SpHtp1$^{24-68}$mRFP(His)$_6$ could be detected under identical conditions (*SI Appendix*, Fig. S3*B*). Interestingly, we found that a modification of H-Tyr(SO_3)-OH with the hydrophobic fluorenylmethyloxycarbonyl (FMOC) group increased the affinity of this compound toward SpHtp1$^{24-68}$mRFP(His)$_6$ ∼fivefold. For both the full-length construct, SpHtp1$^{24-198}$(His)$_6$ and the N-terminal leader mRFP fusion construct, SpHtp1$^{24-68}$mRFP(His)$_6$, very similar binding constants (and thermodynamic parameters) were obtained with this compound of 144 ± 21.9 μM and 116 ± 16.9 μM, respectively (Fig. 3 *A* and *B*). This finding suggests that the protein surface in the SpHtp1 N-terminal polypeptide that is responsible for tyrosine sulfate binding is flanked at least on one side by a hydrophobic surface. Indeed, Fmoc-Tyr(SO_3)-OH was also found to be a better inhibitor of the SpHtp1$^{24-68}$mRFP(His)$_6$ translocation into RTG-2 cells than H-Tyr(SO_3)-OH (*SI Appendix*, Fig. S5). Importantly, the replaced mutant protein construct SpHtp1$^{24-198}$mRFP(His)$_6$GGHLG did not show any interaction to Fmoc-Tyr(SO_3)-OH, demonstrating that the tyrosine-O-sulfate binding properties reside in the N-terminal polypeptide of SpHtp1 (Fig. 3*A*, blue trace).

In summary, the N-terminal leader of SpHtp1 is a peptide from *S. parasitica* that shows host cell-specific translocation. This translocation is independent of phosphoinositol-phosphate, and is instead reliant on sulfate-modified cell-surface molecules. Moreover, our data strongly suggest that the SpHtp1 receptor molecules are tyrosine-O-sulfate modified proteins. Therefore, the translocation of SpHtp1 is clearly different from the process reported for RxLR effectors of plant pathogenic oomycetes (19), which have been reported to bind to phospholipids, and is also distinct from the malaria PEXEL protein translocation process (25–28), because SpHtp1 does not require any pathogen encoded proteins to enter host cells. Tyrosine-O-sulfate–dependent translocation represents a previously undescribed means of effector delivery by oomycetes that may apply to other host-microbe/pest interactions.

Materials and Methods

Detailed descriptions of all methods are given in the *SI Appendix*.

Live Cell Imaging. The cells were incubated with the various recombinant protein constructs in the respective cell type-specific media containing 10% fetal calf sera (FCS). Before imaging, the cells were extensively washed. Microscopy was carried out on a Zeiss LMS 510 confocal microscope, applying identical settings for all samples.

Isothermal Titration Calorimetry. Titration experiments were performed with a MicroCal ITC$_{200}$ at 20 °C. Titrant stock solutions were always prepared with the same batch of buffer as used for dialysis. Because the initial injection generally delivers inaccurate data, the first step was omitted from the analysis. The collected data were analyzed using the program "Origin" (MicroCal) using the binding models provided by the supplier. Errors correspond to the SD of the nonlinear least-squares fit of the datapoints of the titration curve.

Phospholipid Binding. The lipid spot membranes were equilibrated for 10 min with PBS containing 0.1% Tween 20 and 5% lipid free BSA before adding the respective protein constructs. Protein incubations were carried out for 20 min at room temperature. Subsequently, the membranes were extensively washed with PBS/Tween/BSA. Antibody detection was performed with a HRP-coupled anti–His-antibody in (PBS)/Tween/BSA at a titer of 1:10,000 using ECL.

FACS. Equalized cell suspensions were grown to confluent layers. For sulfotransferase inhibition, $NaClO_3$ was added at a final concentration of 70 mM to the medium. After 2 d of growth, the cells were washed and subsequently incubated with the respective protein for 1 h. Subsequently, the cells were dislodged with 1 mL of a trypsin solution and counted. On average a cell concentration of ∼2 × 10^6 cells/mL was obtained. FACS measurements were performed on an LSR II flow cytometer. From 10,000 counted events, a homogenous population of cells was selected and further analyzed for mRFP fluorescence. Data analysis was carried out using FlowJo v 7.6.

Sample Preparation for Western Blotting. Samples were prepared as described for the FACS analysis. After trypsination the cells were harvested by centrifugation and resuspended 2× in PBS to remove the excess of trypsin. The wet cell pellets containing ∼2 × 10^6 cells (∼20 μL) were lysed at 95 °C in 100 μL of Laemmli sample buffer containing 8 M urea, 2% β-mercaptoethanol, and 1 mM PMSF. The sample volume loaded on the gel was 15 μL.

ACKNOWLEDGMENTS. We thank Kevin MacKenzie and Alastair D. McKinnon of the core microscopy facility of the University of Aberdeen; Sharon Kelly for the usage of the CD-spectrometer; Prof. Ian Booth for the use of the iTC200; and Prof. Neil A. R. Gow for helpful suggestions and discussions. This work is supported by the Biotechnology and Biological Sciences Research Council (S.W., P.R.J.B., I.d.B., K.L.M., C.J.S., and P.v.W.), the Natural Environment Research Council (P.v.W.), the University of Aberdeen (S.G., K.L.M., A.J.P., C.J.S., and P.v.W.), the University of Dundee (P.R.J.B.), Rural and Environment Research and Analysis Directorate (S.C.W.), Deutsche Forschungsgemeinschaft TRR 60/1 (to P.B.), Bundesministerium für Bildung und Forschung (A.M. and P.B.), and The Royal Society (P.v.W.). A.J.P. is a co-principal investigator on one grant that funded the research.

1. Birch PR, et al. (2009) Towards understanding the virulence functions of RXLR effectors of the oomycete plant pathogen *Phytophthora infestans*. *J Exp Bot* 60:1133–1140.
2. Hein I, Gilroy EM, Armstrong MR, Birch PR (2009) The zig-zag-zig in oomycete-plant interactions. *Mol Plant Pathol* 10:547–562.
3. Mattoo S, Lee YM, Dixon JE (2007) Interactions of bacterial effector proteins with host proteins. *Curr Opin Immunol* 19:392–401.
4. Stergiopoulos I, de Wit PJ (2009) Fungal effector proteins. *Annu Rev Phytopathol* 47:233–263.

5. Salmond GP, Reeves PJ (1993) Membrane traffic wardens and protein secretion in gram-negative bacteria. *Trends Biochem Sci* 18:7–12.
6. He SY, Nomura K, Whittam TS (2004) Type III protein secretion mechanism in mammalian and plant pathogens. *Biochim Biophys Acta* 1694:181–206.
7. Büttner D, He SY (2009) Type III protein secretion in plant pathogenic bacteria. *Plant Physiol* 150:1656–1664.
8. van West P, et al. (2010) The putative RxLR effector protein SpHtp1 from the fish pathogenic oomycete *Saprolegnia parasitica* is translocated into fish cells. *FEMS Microbiol Lett* 310:127–137.
9. Dou D, et al. (2008) Conserved C-terminal motifs required for avirulence and suppression of cell death by *Phytophthora sojae* effector Avr1b. *Plant Cell* 20:1118–1133.
10. Yaeno T, et al. (2011) Phosphatidylinositol monophosphate-binding interface in the oomycete RXLR effector AVR3a is required for its stability in host cells to modulate plant immunity. *Proc Natl Acad Sci USA* 108:14682–14687.
11. Boutemy LS, et al. (2011) Structures of Phytophthora RXLR effector proteins: A conserved but adaptable fold underpins functional diversity. *J Biol Chem* 286: 35834–35842.
12. Baxter L, et al. (2010) Signatures of adaptation to obligate biotrophy in the *Hyaloperonospora arabidopsidis* genome. *Science* 330:1549–1551.
13. Haas BJ, et al. (2009) Genome sequence and analysis of the Irish potato famine pathogen *Phytophthora infestans*. *Nature* 461:393–398.
14. Phillips AJ, Anderson VL, Robertson EJ, Secombes CJ, van West P (2008) New insights into animal pathogenic oomycetes. *Trends Microbiol* 16:13–19.
15. Tyler BM, et al. (2006) Phytophthora genome sequences uncover evolutionary origins and mechanisms of pathogenesis. *Science* 313:1261–1266.
16. Birch PR, Rehmany AP, Pritchard L, Kamoun S, Beynon JL (2006) Trafficking arms: Oomycete effectors enter host plant cells. *Trends Microbiol* 14:8–11.
17. Rehmany AP, et al. (2005) Differential recognition of highly divergent downy mildew avirulence gene alleles by RPP1 resistance genes from two *Arabidopsis* lines. *Plant Cell* 17:1839–1850.
18. Whisson SC, et al. (2007) A translocation signal for delivery of oomycete effector proteins into host plant cells. *Nature* 450:115–118.
19. Kale SD, et al. (2010) External lipid PI3P mediates entry of eukaryotic pathogen effectors into plant and animal host cells. *Cell* 142:284–295.
20. Dou D, et al. (2008) RXLR-mediated entry of *Phytophthora sojae* effector Avr1b into soybean cells does not require pathogen-encoded machinery. *Plant Cell* 20: 1930–1947.
21. Hiller NL, et al. (2004) A host-targeting signal in virulence proteins reveals a secretome in malarial infection. *Science* 306:1934–1937.
22. Marti M, Good RT, Rug M, Knuepfer E, Cowman AF (2004) Targeting malaria virulence and remodeling proteins to the host erythrocyte. *Science* 306:1930–1933.
23. Grouffaud S, van West P, Avrova AO, Birch PR, Whisson SC (2008) *Plasmodium falciparum* and *Hyaloperonospora parasitica* effector translocation motifs are functional in *Phytophthora infestans*. *Microbiology* 154:3743–3751.
24. Bhattacharjee S, et al. (2006) The malarial host-targeting signal is conserved in the Irish potato famine pathogen. *PLoS Pathog* 2:e50.
25. Chang HH, et al. (2008) N-terminal processing of proteins exported by malaria parasites. *Mol Biochem Parasitol* 160:107–115.
26. Boddey JA, et al. (2010) An aspartyl protease directs malaria effector proteins to the host cell. *Nature* 463:627–631.
27. Boddey JA, Moritz RL, Simpson RJ, Cowman AF (2009) Role of the *Plasmodium* export element in trafficking parasite proteins to the infected erythrocyte. *Traffic* 10: 285–299.
28. Russo I, et al. (2010) Plasmepsin V licenses *Plasmodium* proteins for export into the host erythrocyte. *Nature* 463:632–636.
29. Ellis JG, Dodds PN (2011) Showdown at the RXLR motif: Serious differences of opinion in how effector proteins from filamentous eukaryotic pathogens enter plant cells. *Proc Natl Acad Sci USA* 108:14381–14382.
30. Farzan M, et al. (1999) Tyrosine sulfation of the amino terminus of CCR5 facilitates HIV-1 entry. *Cell* 96:667–676.
31. Kehoe JW, Bertozzi CR (2000) Tyrosine sulfation: A modulator of extracellular protein-protein interactions. *Chem Biol* 7:R57–R61.
32. Yu Y, Hoffhines AJ, Moore KL, Leary JA (2007) Determination of the sites of tyrosine O-sulfation in peptides and proteins. *Nat Methods* 4:583–588.
33. Choe H, et al. (2005) Sulphated tyrosines mediate association of chemokines and *Plasmodium vivax* Duffy binding protein with the Duffy antigen/receptor for chemokines (DARC). *Mol Microbiol* 55:1413–1422.
34. Wilkins PP, Moore KL, McEver RP, Cummings RD (1995) Tyrosine sulfation of P-selectin glycoprotein ligand-1 is required for high affinity binding to P-selectin. *J Biol Chem* 270:22677–22680.
35. Liu S-L, et al. (2011) Visualizing the endocytic and exocytic processes of wheat germ agglutinin by quantum dot-based single-particle tracking. *Biomaterials* 32:7616–7624.
36. Chang WC, et al. (2009) Incorporating support vector machine for identifying protein tyrosine sulfation sites. *J Comput Chem* 30:2526–2537.